

Objective Evaluation of Whole Body Kinematics in a Simulated, Restrained Frontal Impact

JEREMY M. SCHAP, BHARATH KOYA, and F. SCOTT GAYZIK 

Wake Forest University School of Medicine, Virginia Tech-Wake Forest University Center for Injury Biomechanics,
575 N Patterson Ave, Biotech Place, Suite 120, Winston Salem, NC 27101, USA

(Received 25 June 2018; accepted 29 November 2018; published online 6 December 2018)

Associate Editor Estefanía Peña oversaw the review of this article.

Abstract—The use of human body models as an additional data point in the evaluation of human-machine interaction requires quantitative validation. In this study a validation of the Global Human Body Models Consortium (GHBMC) average male occupant model (M50-O v. 4.5) in a restrained frontal sled test environment is presented. For vehicle passengers, frontal crash remains the most common mode, and the most common source of fatalities. A total of 55-time history traces of reaction loads and kinematics from the model were evaluated against corresponding PMHS data ($n = 5$). Further, the model's sensitivity to the belt path was studied by replicating two documented PMHS cases with prominent lateral and medial belt paths respectively. Results were quantitatively evaluated using open source CORA software. A tradeoff was observed; better correlation scores were achieved on gross measures (e.g. reaction loads), whereas better corridor scores were achieved on localized measures (rib deflections), indicating that subject specificity may dominate the comparison at localized anatomical regions. On an overall basis, the CORA scores were 0.68, 0.66 and 0.60 for force, body kinematics and chest wall kinematics. Belt force responses received the highest grouped CORA score of 0.85. Head and sternum kinematics earning a 0.8 and 0.7 score respectively. The model demonstrated high sensitivity to belt path, resulting in a 20-point increase in CORA score when the belt was routed closer to analogous location of data collection. The human model demonstrated overall reasonable biofidelity and sensitivity to countermeasures in frontal crash kinematics.

Keywords—Human body model, Finite element, Validation, Frontal impact, Injury, Biomechanics.

INTRODUCTION

Despite advances in the field, vehicle crash remains a major public health problem worldwide. The latest US data (2016) indicates that 37,461 deaths were attributed to vehicular traffic accidents, an increase of 5.6% over the previous year,³¹ continuing an increasing trend dating back to 2013. Globally, road traffic injuries are estimated to be the 8th leading cause of death and the leading cause of death for those aged 15–29.⁵² These statistics reflect all modes of travel, but vehicle passengers are by far the most represented in fatal and nonfatal injury when using exposure-based methods to quantify risk of injury or death from vehicular crash.⁷ For vehicle passengers, frontal crash is the most common mode for fatalities accounting for roughly 45% of all car crash fatalities.⁶ Injuries to the head and chest are the two most common drivers of death following vehicle crash.¹⁰ A recent study analyzing NASS data from frontal impacts with late model vehicles and belted occupants, found a similar pattern for AIS 3 + injuries,⁹ underscoring the need for further improvement of safety systems.

Biofidelic human surrogates are an essential part of improving vehicle safety systems. Such surrogates include Post Mortem Human Subjects (PMHS), Anthropomorphic Test Devices (ATDs, i.e. crash test dummies), and computational human body models (HBMs). The cost and time associated with PMHS procurement, along with a relative lack of available specimens, and high variability in terms of age, weight, bone quality, and co-morbidities makes it difficult to use PMHS as the de-facto solution for full body scale biomechanics studies or compliance testing. Therefore, researchers often turn to ATDs and HBMs. While ATDs serve as the foundation of injury biomechanics regulation, there are limits to the data they can provide

Address correspondence to F. Scott Gayzik, Wake Forest University School of Medicine, Virginia Tech-Wake Forest University Center for Injury Biomechanics, 575 N Patterson Ave, Biotech Place, Suite 120, Winston Salem, NC 27101, USA. Electronic mails: jschap@wakehealth.edu, bkoya@wakehealth.edu, sgayzik@wakehealth.edu

when analyzing whole body kinematics in vehicle crash. A recent study comparing state of the art ATDs to PMHS in a frontal crash sled environment found kinematic agreement using the ISO/TS 18571 standard for objective time history signal evaluation in the 0.55 range, with 1 being the best score.¹ A central hypothesis of this work is that an HBM can demonstrate equal or improved performance when time history data is compared to PMHS.

Computational human models offer inherent characteristics that make them an attractive counterpart to traditional Anthropometric Test Devices (ATDs, or dummies) and PMHS. These include the well documented notions of cost savings and improved anatomical representation of vehicle occupants.

The Global Human Body Models consortium average male HBM is used in this study. The geometry of the body was derived from a multi-modality imaging protocol of a living subject meeting numerous anthropometric criteria.^{16,17} A distributed development paradigm was used with body region centers of excellence performing regional validation. This included studies of the head,^{28,45,53} neck,^{5,13,14,29,30} thorax,^{25,26,36} abdomen^{8,44} and pelvis²² and lower extremity.^{41,46,54,55} At the full body level, studies on organ location,²⁰ mass distribution,⁵¹ chest band data validation,²¹ and lateral and thoracic hub validation have been conducted.^{33,47,50}

The use of HBMs as an additional data point in the evaluation of human machine interaction requires quantitative validation of the time history data derived from these models. The GHBMC models have also been used to evaluate and compare various objective evaluation software schemes.⁴⁸ However, there have been relatively few studies specifically documenting its whole body kinematics in frontal crash. One such work studied the kinematic response of the GHBMC M50-O model against low (3.3 m/s) and high (6.7 m/s) velocity frontal sled tests at 5 locations (head, T1, sternum, T12 and sacrum).² Resultant data were reported along with objective evaluations scores indicating fair to good results. However, comparisons were limited to resultant motion paths, and detailed data on chest deformation were not reported.

Given the aforementioned epidemiological motivation, data from a frontal sled test performed using five male PMHS (age, stature, body weight and BMI range of 37–76 years, 1.78–1.84 m, 68–88 kg, 21.7–27.5)³⁹ were selected as the basis for the validation reported herein. In this experimental work, the sled seat pan was rigid (steel) and the buck did not utilize any airbags or advanced countermeasures, such as seatbelt pretensioners. For each PMHS test run, the sled was decelerated from a velocity of 40 km/h. Three-dimensional thoracic kinematic data and load cell data were col-

lected and have been extensively published, including corridors for model evaluation.^{3,4,11,24,39} Due to the well documented correlation between belt path and injury location,²³ the data set was furthermore selected because sensitivity to belt path could be studied within the FEA model.

In summary, the purpose of the study was to validate a full body FEA model in a well-documented laboratory frontal sled condition. Specifically, the kinematics and kinetics of the simulated occupant in restrained frontal crash are evaluated. A secondary goal was to perform a sensitivity study, based on reported data, to examine the effect of belt path variance at 5 discrete locations on the chest. For the belt path study, our hypothesis was that the HBM would show similar trends as reported in the experimental data based on belt path.

MATERIALS AND METHODS

This section details the methods employed for conducting simulations of an average male FEA model in a restrained frontal impact. A total of 3 simulations were conducted, a baseline condition and two additional simulations in which the belt path was varied based on published data from Shaw *et al.* Data used in this study were obtained from the following sources. The experimentalists who conducted the PMHS work provided digital copies of the previously-published corridors used for PMHS response [37–38] as well as the FEA model of the buck.³⁸ The HBM used was the GHBMC M50-O v. 4.5 (average male detailed occupant model), it was obtained *in-house* as part of ongoing research efforts. All simulations were performed with MPP LS-Dyna R7.1.2 in a high-performance cluster environment. Fracture in cortical bone was enabled through element deletion but analysis in this work is limited to kinematics and kinetics, not injury prediction.

Boundary Condition

The seat buck, excluding the seat belts, were modeled as rigid. Two pre-simulations were conducted to position the model as follows. In an initial simulation, the M50-O hands were lowered to the thighs and the legs were slightly extended to match the posture documented.³⁹ Then, the model was gravity settled onto the virtual representation of the buck.³⁷

Figure 1 shows the surfaces defined for each of the reaction force and seatbelt load cells. The seat pan, foot pan, and knee bolster load cells were modeled using a force transducer contact option. Chest kinematics were calculated relative to a local coordinate

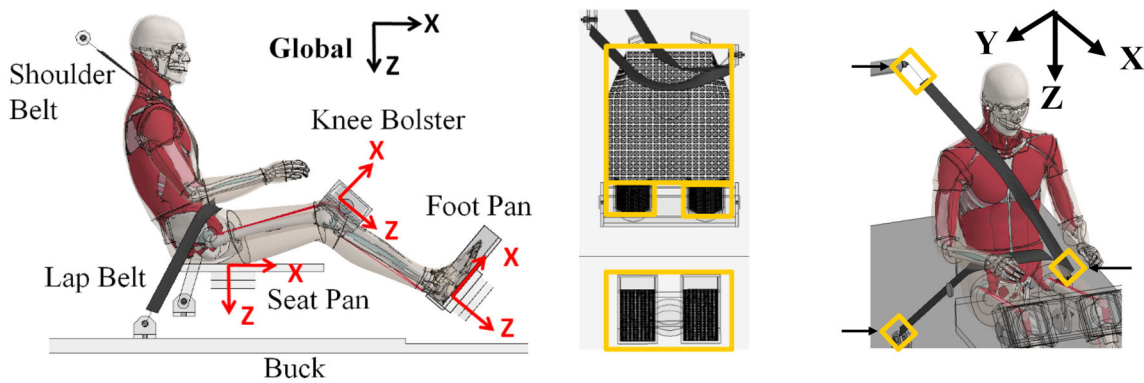


FIGURE 1. Model set up, baseline condition. Global coordinate system defined in SAE J1733 convention and local coordinate systems for reaction load outputs; the Y axis (not shown) points out of the page for all coordinate systems (left figure). Location of force transducers (center) and seat belt load cell sensors (right) showing upper shoulder belt (USB), lower shoulder belt (LSB) and lap belt (LB).

system modeled on the T8 vertebra in the SAE J1733 local coordinate system in accordance with the experiment.³⁹ The global coordinate system for kinetic and kinematic data output was modeled according to the SAE J1733 local coordinate system shown in Fig. 1.⁴³

Following gravity settling, shoulder and lap seatbelts were created using LS-PrePost's occupant seatbelt fitting tool function (LSTC, Livermore, CA). The 1D and 2D seatbelt material properties of the model were based on the experimental seat belt specifications. In the aforementioned publication, a gridded plot of belt path was provided for each subject showing the location of the belt centerline relative to anatomical landmarks. The landmarks were readily identified on the FEA model. The data was used to route the baseline belt path relative to reported anatomical landmarks. A path representative of the majority of the specimens was replicated, which was over the sternum and lower left (LL) landmarks (Fig. 2). Shoulder and lap seatbelt elements at the locations of the instrumentation were used to collect belt forces (Fig. 2). The material model used in the simulation for seatbelt elements can be found in the supplemental data in Appendix C.

Validation Simulation

An initial and constant velocity of 11.82 m/s was applied to the entire model in the X direction (forward motion) for the first 100 ms during which stress developed between the HBM and the rigid seat *via* gravity. This period of constant velocity motion allowed for additional settling and better coupling to the buck. The contact force at the seat pan was 0.69 kN at the close of this settling period, which corresponds to 91% of the model's body weight. The additional reaction force due to body weight unaccounted here was through the leg support. The contact

force had leveled off at the close of this 100 ms settling window indicating a steady state. Immediately following this, a 150 ms deceleration pulse (Fig. A7), was integrated and applied as a velocity vs. time curve to the sled. The mean pulse reported by Shaw *et al.* was used to decelerate the buck.³⁹ Gravity remained active throughout the simulation. To avoid seat belt slack before the deceleration pulse and to match the hand-tightened pretension on the seat belts in the experiment, the upper shoulder belt and lap belt were pretensioned to 10 and 50 N, respectively.

Validation Data Preparation

All data used in validation ($n = 5$ PMHS) have been published.²⁹ These tests are also available on a publicly accessible biomechanics database hosted by NHTSA¹ (Table 1). The M50-O body mass and stature is within 0.3 and 1.7% of the average body mass and stature of the PMHS, respectively. Table 1 provides basic anthropometry of each specimen along with the respective percentile for each measure. The model's biofidelity was evaluated across 55 kinetic and kinematic responses. For each signal response, the mean corridor was developed as the average of the data while the upper and lower corridors were developed as ± 1 standard deviation. No model data scaling was performed because the average mass and height of the PMHS and the M50-O mass were comparable, and to align with previous studies which have published corridors from this work, which were also unscathed.^{3,11}

Data Processing Procedures

Kinematic and load cell data were output from the simulation at 10 kHz. Seatbelt data was extracted from

¹<https://www.nhtsa.gov/research-data/databases-and-software>.

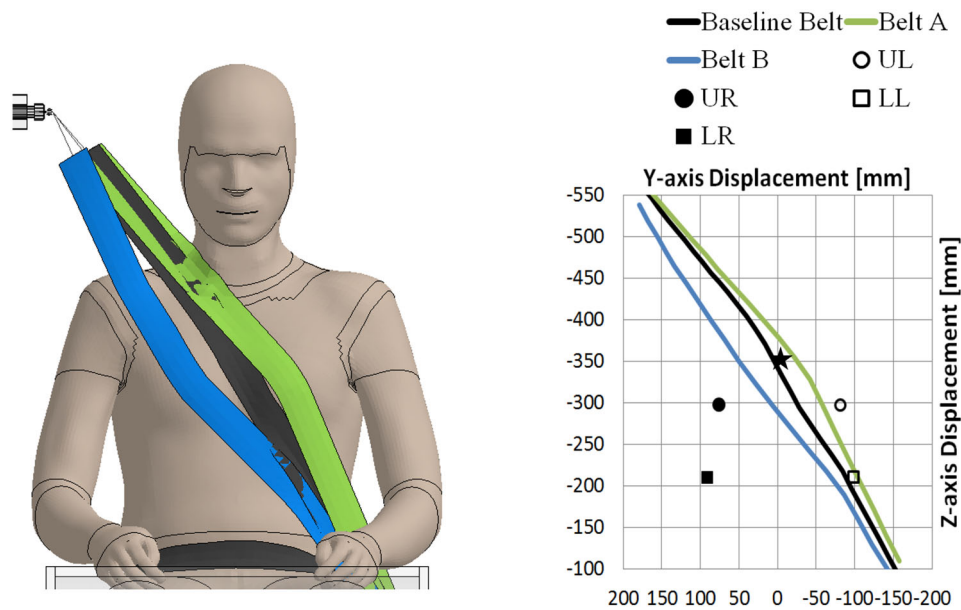


FIGURE 2. Baseline, Belt A, and Belt B shoulder belt paths. Belt path on HBM (left) and belt path relative to chest sensors (right).

TABLE 1. PMHS used for HBM biofidelity assessment.²⁹

Subject	Age (years)	Body mass (kg)	Body mass percentile (%)	Stature (m)	Stature percentile (%)	BMI (kg/m ²)
PMHS 1294	76	70	22.5	1.78	65	22.1
PMHS 1295	47	68	17	1.77	59.5	21.7
PMHS 1378	72	81	61	1.84	89	23.9
PMHS 1379	40	88	81	1.79	69	27.5
PMHS 1380	37	78	51	1.80	75	24.1
Average PMHS	54 ± 18	77 ± 8 kg	46.5 ± 24	1.80 ± 0.03 m	71.5 ± 10	23.9 ± 2.0
GHMBC	–	77 kg	44	1.77 m	59.5	24.6

Percentiles of mass and stature are included from Gordon *et al.*

the one-dimensional seatbelt elements near the analogous of load cells in the experimental work (Fig. 1). As performed in the experiment, kinetic data was filtered with channel frequency class (CFC) 60 according to the SAE J211 filter standard.^{4,42} The velocity of the buck was subtracted from each X displacement response to represent relative displacement. The data output for the first 100 ms of the simulation before the deceleration pulse was removed and the data for comparison to the PMHS data began at time = 0. The foot pan and knee bolster load cell model data were transformed from the global coordinate system to each respective local coordinate system shown in Fig. 1.

Belt Path Sensitivity

Two additional simulations were run to assess belt path sensitivity. The baseline shoulder belt was removed and two additional shoulder belts were created. Each belt path was created to match data from the belt paths reported by Shaw *et al.*^{4,39} as was done

for the baseline belt path; by leveraging reported data of belt path relative anatomical landmarks. Two PMHS belt paths which prominently displayed a more lateral or medial trajectory from the baseline belt were selected. The two belt path variations are henceforth referred to as Belt A (25 mm leftward at sternum level) and Belt B (50 mm rightward at sternum level). The Belt A and Belt B paths were created based on the belt path of PMHS 1358 and PMHS 1359, respectively.³⁹ Shoulder belt connection points remained the same as in the baseline belt. Fig. 2 shows the belt path of the baseline belt, Belt A, and Belt B on the HBM in the coronal plane. For each simulation, the local coordinate system X direction (Anterior-to-Posterior chest compression) was analyzed. Responses were quantitatively assessed and compared to baseline.

Objective Evaluation

Correlation and Analysis (CORAs) v3.51,¹⁸ was run to objectively evaluate the M50-O response with re-

spect to the PMHS data for each signal response. The response was quantified with a score between 0 and 1, with 1 representing a perfect match and 0 representing a poor match. More background on the use of CORA in human body modeling is described by Davis *et al.* and Vavalle *et al.*^{12,48} The score is based on a combined corridor and cross-correlation score. The inner corridors utilized for the corridor score are the ± 1 standard deviation corridors from the experiments by Shaw *et al.* The outer corridors were ± 2 standard deviations.

The CORA parameters used for this study are provided in the Appendix (Table A1). Note that the full time history (from time = 0 to 150 ms) was evaluated to assess how well the mass recruitment and kinematics tracked with the onset of loading due to velocity change. Typically, when averaging CORA scores from multiple signals of the same sensor, the CORA score for each signal is equally weighted. However, the overall quality of the model response may be distorted when one axis signal produces a significantly higher response in terms of magnitude compared to another axis signal of the same sensor. For instance, in this validation case, the mean corridor's peak magnitude of the first thoracic vertebra displacement in the direction of sled motion, the X direction, is 3.5 times that of the lateral displacement, the Y direction. Therefore, a weighting factor was used, the Signal Magnitude Factor.¹² SMF-derived weights were assigned to each output signal. The sum of the SMF values for a given sensor is always 1. The SMF is calculated by taking the absolute peak value of one channel within an orthogonal set, normalized by the sum of the peaks of all signals for a given sensor (typically X , Y and Z components, $n = 3$) as shown in Eq. (1). The calculated SMF for each signal is shown in the Appendix in Table A2.

$$\text{SMF} = \frac{R_i}{\sum_i^n R} \quad (1)$$

CORA scores for the full body model in the baseline belt condition are provided. The CORA scores for the belt sensitivity study are provided for the measures related to chest motion only.

RESULTS

General Trends—Baseline Condition

The HBM postural data at the instant prior to the initiation of the pulse is found in Appendix B. Time history response plots are provided in the supplemental material for all data points (Figure A1 through Figure A5). The general trend of the PMHS is captured in

most instances, with notable deficiencies in the Y (medial to lateral) directions. Correlation scores are provided in Table 2. The overall force CORA score was 0.68, the overall kinematic CORA score (excluding chest data) was 0.66, and the overall chest kinematic CORA score was 0.60. The corridor, shape, size, phase, and CORA score for each signal response are shown in Table 2 and are color-coded based on the score. Corridor scores are lower, reflecting tighter corridors and low variability within the experimental signals. A graphical history of the event can be found in Fig. 3.

Load Cells—Baseline Condition

Considering all the load cells, the belt force responses received the highest grouped CORA score of 0.85. The three belt force responses quite accurately match the corridors, including the most relevant parts of the signal from ramp-up to peak loading. The unloading of the belt is slightly faster in the model than the experimental mean, suggesting a slightly more elastic response than the PMHS. Like the experimental data, the upper shoulder belt exhibited the greatest load, following by lower shoulder belt and finally lap belt. The lap belt load is substantially lower than typical frontal crash lap belt loads due to the atypical restrains on the subjects' lower extremities.

The lower lap belt load manifests in rather high knee forces. These represent contact with a knee restraint from a very early stage (around 15 ms). Unlike impact forces there is a relatively gradual rise to a peak, since the knees are effectively in contact with these restraints for the duration of the event. The bimodal response is captured very well in the model and is likely to due an initial load from recruitment of the body mass through the femur, and a secondary load from when the upper body reaches peak forward displacement. The orthogonal direction in the feet Z , and knee X dominate the response. The peak force responses in the X and Z directions, the plane of motion, closely matched the corresponding experimental peaks. However, there was a small delay in the model peaks for the perpendicular (Z) foot and seat forces, resulting in lower corridor scores. These are likely due to slight deviations in the settling of the model vs experiment.

Kinematics—Baseline Condition

The kinematics results are presented first for the body kinematics excluding the five signals of the ribcage. The body kinematic shape and phase scores which were each 0.89 were noticeably higher than the size score (0.60). This is also reflected in the corridor score.

TABLE 2. Weighted CORA scores for biofidelity assessment, green indicates higher score, baseline condition.

Response type	Signal	Corridor score	Cross-correlation				Overall CORA score
			Shape	Size	Phase	Combined ^a	
Forces	Belt forces	0.72	0.96	0.97	1.00	0.98	0.85
	Seat Z	0.26	0.56	0.56	1.00	0.71	0.48
	R knee	0.50	0.83	0.91	1.00	0.91	0.71
	L knee	0.52	0.83	0.72	1.00	0.85	0.68
	Foot	0.47	0.89	0.93	0.88	0.90	0.69
	Average	0.49	0.81	0.82	0.98	0.87	0.68
Kinematics	Head	0.74	0.99	0.59	1.00	0.86	0.80
	R shoulder	0.57	0.76	0.87	0.89	0.84	0.71
	L shoulder	0.27	0.98	0.45	1.00	0.81	0.54
	T1	0.23	0.93	0.46	0.81	0.73	0.48
	T8	0.43	0.96	0.56	0.89	0.80	0.62
	L2	0.75	0.95	0.66	0.87	0.83	0.79
	L4	0.70	0.81	0.76	0.85	0.81	0.75
	Pelvis	0.59	0.72	0.41	0.82	0.65	0.62
Average	0.53	0.89	0.60	0.89	0.79	0.66	
Chest Kinematics	Sternum	0.75	0.80	0.57	0.65	0.67	0.71
	Upper left chest	0.71	0.86	0.28	0.85	0.66	0.68
	Upper right chest	0.46	0.53	0.17	0.59	0.43	0.44
	Lower left chest	0.70	0.67	0.34	0.67	0.56	0.63
	Lower right chest	0.59	0.65	0.38	0.43	0.49	0.54
Average	0.64	0.70	0.35	0.64	0.56	0.60	

^a(Shape + Size + Phase)/3

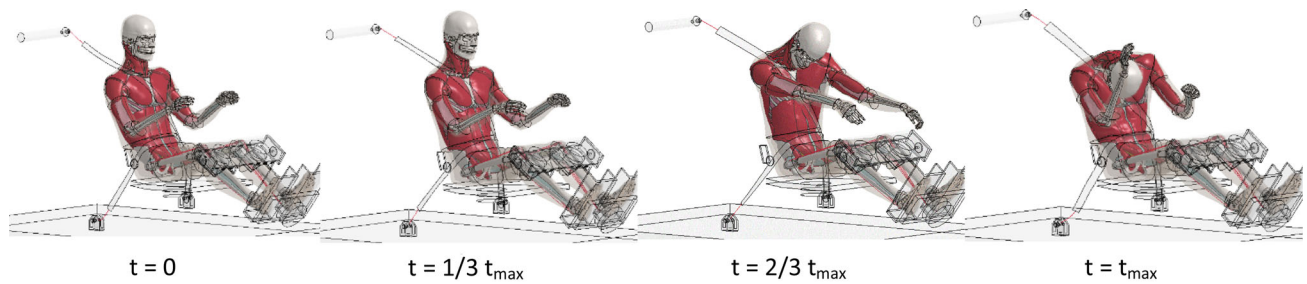


FIGURE 3. Time history of the simulated event, baseline condition.

Thus, the trends were captured but slightly underestimated by the model. In the spine data, the model underestimated motion in the YZ -plane for the more superior locations. The T1 vertebra received the lowest corridor score of 0.23, particularly since the model X displacement, which contributed to 67% of the overall weighted T1 vertebra score, fell short of the experimental lower corridor for most of the time. Conversely, the head motion received the highest score in the kinematics results, with a score of 0.80. The sternum achieved the highest chest kinematic CORA score of 0.71. In terms of magnitude of motion, and like the experimental data, the model exhibited that the upper body kinematics were much larger than data than the lower body kinematics because the lower extremity was restrained. The head exhibited the largest resultant motion and was among one of the best predicted metrics. The model underpredicted the lateral motion across all kinematic signals, and this likely contributed to the underestimate of the left (free) shoulder motion.

The design of the PMHS study was intended to focus on dynamic thoracic loading, and thus there were five signals collected at specific locations of the ribcage. These included the sternum (mid-body), two upper chest landmarks located on the 4th rib at the costal cartilage junction, and lower chest landmarks located on the confluence of the 7th and 8th ribs at the junction of the costal cartilage. The locations of these points were selected based on the experimental description. Similar to the experimental data, the vast majority of the deformation was found to be the X or anterior-posterior direction. As noted in Fig. 2, the measurement locations nearest to the belt path were quite well estimated by the model (left side and sternum) while the right side was underestimated. The belt sensitivity work elucidates some trends regarding the measurement location vs. belt path.

Shoulder Belt Path Sensitivity

The comparison of CORA scores for only the anterior-posterior chest compression responses (local

X direction) of each belt path can be found in Table 3. The average CORA score was 0.76, 0.77, and 0.76 for the baseline, Belt A, and Belt B belt paths, respectively. Upper level data points showed the large differences in CORA between different belt paths at the same sensor location. The baseline upper left chest X compression score was 0.79, 21 points higher than the corresponding Belt B (25 mm leftward shift) score of 0.58. Similarly, the Belt B (50 mm rightward shift) score for upper right chest X compression was 0.70, 20 points higher than the corresponding Baseline score of 0.50. In both cases, the belt path was moved closer to the point of measurement. The overall average CORA scores of all measures were unaffected by the belt path sensitivity and thus the analysis is focused on the chest locations only.

DISCUSSION

The test series that formed the basis for this comparison was selected due to the large amount of time history validation data reported by the experimentalists ($n = 55$). The tests employed an atypical design that was intended to focus on thoracic deformation (Shaw *et al.*) The utility of the data set for model validation outweighed any question of whether or not the experimental design created loading similar what occupants experience in real world frontal crash. In short, the key was to compare the response of the GHBMCM50-O model in a matched simulation. The focus of the experiments on thoracic deformation further motivated the belt sensitivity simulations presented. There are a number of consequences of this test design, including lower than usual lap belt load and arrested pelvic kinematics. These were also observed in the model. This did not prevent us from comparing reaction loads of the lower extremity, which showed quite good agreement overall to the experimental data.

The study shows that the model is a viable surrogate for human body kinematics and kinetics in this restrained frontal crash sled environment. The 55 data traces found the Appendix indicate that the model

TABLE 3. Anterior–Posterior compression as a function of belt path, through CORA scores.

Signal	Baseline	Belt A	Belt B
Sternum X	0.83	0.84	0.85
Upper left chest X	0.79	0.91	0.58
Upper right chest X	0.50	0.43	0.70
Lower left chest X	0.86	0.86	0.91
Lower right chest X	0.80	0.81	0.78
Average	0.76	0.77	0.76

Green color indicates higher scores. Belt A represents a 25 mm leftward shift at the sternum level and Belt B represents a 50 mm rightward shift at the sternum level. Belts were designed to match observed maxima in the experimental data

generally matches the kinematic and kinetic data trends exhibited by the PMHS data. This includes some notable exceptions in the Y direction (lateral-medial) which should prompt users to more closely study the modeling approach of the spine, particularly in the thoracic spine area. However, the CORA scores indicate, quite good agreement in shape and phase in particular. As indicated by the size score, some of these trends fail to match the magnitude of displacements seen in the PMHS indicating an overall slightly stiffened response, particularly in the thoracic spine. Table 2 is arranged from gross measures (e.g. force) and to more localized measures, chest kinematics. In general, the cross correlations scores are better than the corridor scores for gross measures but the reverse is true for the chest kinematics. This is generally due to corridor width. Closely matched cadavers in a well-controlled experiment can produce very tight corridors for gross measures, like knee reaction loads, but anatomical variation begins to blur the results when looking at individual rib motion. Better agreement was observed among cross correlation scores in kinetics (e.g. belt loads, reaction forces) but those scores lowered as a more localized comparison was made. Importantly, the head and chest (as measured at the sternum) showed very good agreement with the experimental data, with overall CORA scores of 0.80 and 0.71 respectively. The anterior-posterior rib compression showed also reasonable correlation with only one measure among the six achieving a CORA score < 0.7 for all belt variations (Table 3).

The anatomical basis of the human model, with a detailed representation of the rib cage and costal cartilage, was shown to be of high value to the biofidelity of the model, as noted by belt sensitivity. Right or left movement of the belt trajectory towards the location of data collection in the experiment, improved CORA

scores by roughly 20 pts (Table 3, Fig. 2, Fig. A6). The two locations most consistently near the path of the belt (sternum and lower left, Fig. 2, Fig. A6) showed the best agreement. The upper right and lower right chest measures were farthest from the belt and showed some of the poorest CORA scores. There are implications of these results for future modeling studies. The most common skeletal injury that a restrained occupant will sustain during a frontal collision is rib fractures,³⁴ making them a highly studied aspect in human modeling. Rib failure was modeled in the M50-O through element erosion with a failure plastic strain thresholds of 0.018 and 0.13 for cortical and trabecular bone, respectively.¹⁹ While rib fracture was beyond the scope of the current study, the results here indicate that simply varying the belt path to match the experimental conditions will change the overall deformation and thus strain, and should be undertaken when assessing the likelihood of rib fracture.

There is evidence in the literature to suggest that the level of agreement (as interpreted by the CORA score) is favorable when compared against similar studies using state of the art ATDs. A recent study of an ATD to PMHS comparison that used CORA to evaluate agreement resulted in scores between 0.44 and 0.65.³⁵ That study analyzed an underbody blast condition at 4 m/s with times to peak velocity ranging from 5 to 10 ms.

Given that the “gross” measures of force from the model tended to agree best with the experimental results in terms of peaks and timing indicates that the mass distribution, joint modeling approach, and geometry of the M50-O model are quite reasonable. There are several potential factors that may contribute to better matches in the future for more localized data points. One method which has been attempted is to more precisely match the posture of each PMHS tested

with the model and then average the responses. However, in a previous study, this frontal sled case was used to study the effect of initial seated posture on kinetic and kinematic results in the THUMS human model.³⁷ In that study, the human model was run once for each initial posture of the PMHS used to calculate the CORA ratings. Results in the study showed that changing the initial posture significantly affects individual signal responses, but the overall CORA score does not significantly change. While individual anatomical variation surely also plays a role, our goal was to compare the GHBMCM50-O model as a standard to the mean experimental data, in much the same way as an ATD may be compared to a set of PMHS data. This is motivated by the fact that many users of human models use only the standard anthropometry as originally developed. Finally, when simulating a complex environment such as this, slight deviations between the actual buck and the model of the sled environment itself may also play a role.

There is some artificial spine stiffness evident in that the model tends to under predict the peak displacement. The lumbar spine produced a comparatively high CORA scores indicating perhaps a cumulative effect as one traverses the spine superiorly. T1 and T8 produced the lowest CORA scores within the spine. The *X* direction (anterior–posterior) model responses of the T1 and T8 under-predict the motion of the corresponding corridors. The GHBMCM50-O v. 4.5 spine is composed of a series of rigid bodies interconnected with zero-length, 6 degree of freedom beams with force deflection response profiles taken from literature.³² While a reasonable approach, further elongation in the cranial-caudal dimension at high forward flexion could potentially be achieved through explicit modeling of the thoracic spine to include intervertebral disks and key anterior and posterior ligaments. The GHBMCM50-O spine also failed to generate the “wave like” motion observed in PMHS, moving first left and then right. It should be noted that the magnitudes of these motion traces were small compared to what was observed in the sagittal plane (Fig. A2). While it has been shown that the model has good biofidelity in full body validation cases,⁴⁹ the data here in the *Y* dimension are highly local and more subtle (± 20 mm) than the previous studies.

Some limitations of this study should be noted. Previous studies have shown that model morphing can improve correlation with experimental data.^{12,40} However, our goal in this work was to use the corridors published to assess the GHBMCM50-O model as a standard. The anthropometry of the PMHS used as the basis for the validation presented in this paper is summarized in Table 1. While the mean percentiles of the subjects closely agreed with the GHBMCM model

itself, and efforts were made to utilize only specimens that were as close as possible the median, there were significant differences in body mass percentile among the specimens. This is a common limitation among PMHS studies. The consequences of mass variation likely are the main drivers behind the divergence of the kinetic signals at the peaks.

The corridors used in the study were developed from mean and standard deviation of the experimental data. Corridor methods in injury biomechanics vary widely from very simplistic such as a method used by Ghery *et al.* which calls for a simple 5 and 50% of the peak load in the absence of other data,¹⁸ to scaling and alignment based on a percent of the peak,²⁷ to more advanced methods such as point-wise normalization.¹⁵ However, in the latter study at least, this method was used in part to remove phase differences that may have been introduced when combining data from multiple laboratories. Furthermore, that method only operated over what was deemed the loading portion of the curve, which may not be relevant to the current study. Lastly, the corridors used in this work are the same as those presented by the experimentalists in order to facilitate comparison of these results with the recent paper published on the PMHS tests modeled.

GHBMCM50-O model’s initial posture was compared against the reported experimental mean posture (Appendix B). The greatest deviation from the mean experimental value was found in the pelvic angle (it was coincidentally the greatest variation observed in the experiment). There are mitigating circumstances that lessen the impact of this difference on our results. In the Shaw 2009 paper, it is noted that, “The head and back support, comprised of a matrix of adjustable cables, and the upper shoulder belt anchor were adjusted to achieve a typical occupant seated posture and corresponding relationship of shoulder to shoulder belt.” The final posture achieved by the model in our work similarly represents a typical occupant seated posture. Also, like the experimentalists, the model was settled into the buck without making any specific manipulations of the hips. Finally, given the restrained lower extremity, it is unlikely that this pelvic angle would considerably affect the response since overall pelvic and lower extremity motion was arrested by the support structure employed.

Despite not exploring anatomical or postural variation, this study found that the initial belt path significantly affects chest compression responses. In future PMHS data collection, if imaging and surface contour data are made available from each subject, it would be possible to use existing morphing techniques to match subjects.⁴⁰ Age effects were also not included because the standard GHBMCM model was used as the basis for the study. The age of the model is considered

varied since the original geometry source is a 26-year-old male¹⁶ while material properties encompass a wide range of sources of literature.³⁸ The age of the PMHS used in the Shaw study ranged from 37 to 76 years with a mean age of 54 ± 18 years. Further study of age and its effects were considered beyond the scope of the work.

Future work should be focused on assessing the improvement of correlation after either morphing the GHBMC model to specific PMHS anthropometries contained in this set, or alternatively performing *post-hoc* scaling of the PMHS data itself. Should these efforts be undertaken, a reasonable attempt at capturing the effect of age of each specimen given the range of ages of the PMHS used should also be included. Thus the objective evaluation values presented here should be considered a baseline, that could improve further with more refinement of the comparison.

In conclusion, the M50-O v4.5 GHBMC model was simulated in an 11.8 m/s frontal sled impact to assess its biofidelity. Fifty-five data traces were compared to PMHS data and are provided in the supplemental material. The CORA scores were highest for shape and phase, with size being somewhat underestimated. Gross measures of reaction loads showed good agreement. Good agreement was found in the reaction loads, head and sternum kinematics. The upper spine motion was underestimated. Seatbelt path was found to be a driver of agreement with the data, and routing the belt path closer to the point of measurement was found to greatly improve CORA scores for the upper chest data points.

ELECTRONIC SUPPLEMENTARY MATERIAL

The online version of this article (<https://doi.org/10.1007/s10439-018-02180-2>) contains supplementary material, which is available to authorized users.

ACKNOWLEDGMENTS

This work was supported by the Global Human Body Models Consortium, LLC, under GHBMC Project No. WFU-006. All simulations were run on the DEAC cluster at Wake Forest University, with support provided by Adam Carlson and Cody Stevens. The authors gratefully acknowledge the contributions of GHBMC developers, including: L. Zhang (Wayne State), D. Cronin (U. Waterloo), M. Panzer (U. Virginia), P. Beillas (U. Lyon). Dale Johnson (WFU) assisted in manuscript preparation.

CONFLICT OF INTEREST

F Scott Gayzik is a member of Elemance, LLC., which distributes academic and commercial licenses for the use of GHBMC-owned computational human body models.

REFERENCES

- ¹Albert, D. L., S. M. Beeman, and A. R. Kemper. Occupant kinematics of the Hybrid III, THOR-M, and postmortem human surrogates under various restraint conditions in full-scale frontal sled tests. *Traffic Inj. Prev.* 19:S50–S58, 2018.
- ²Arun M., J. Humm, N. Yoganandan and F. Pintar. Biofidelity Evaluation of a Restrained Whole Body Finite Element Model under Frontal Impact using Kinematics Data from PMHS Sled Tests In: *IRCOBI*. Lyon, France, 2015.
- ³Ash J., D. Lessley, J. Forman, Q. Zhang, G. Shaw and J. R. Crandall. Whole Body Kinematics: Response Corridors for Restrained Frontal Impacts. In: *IRCOBI Conference*. Dublin, Ireland, 2012.
- ⁴Ash, J., G. Shaw, D. Lessley, and J. R. Crandall. PMHS restraint and support surface forces in simulated frontal crashes. *Int. J. Automot. Eng.* 4:41–46, 2013.
- ⁵Barker, J. B., D. S. Cronin, and R. W. Nightingale. Lower cervical spine motion segment computational model validation: kinematic and kinetic response for quasi-static and dynamic loading. *J. Biomech. Eng.* 139:16, 2017.
- ⁶Bean, J. D., C. J. Kahane, M. Mynatt, R. W. Rudd, C. J. Rush, and C. Wiacek. Fatalities in Frontal Crashes Despite Seat Belts and Air Bags. Washington: National Highway Traffic Safety Administration, 2009.
- ⁷Beck, L. F., A. M. Dellinger, and M. E. O'Neil. Motor vehicle crash injury rates by mode of travel, united states: using exposure-based methods to quantify differences. *Am. J. Epidemiol.* 166:212–218, 2007.
- ⁸Beillas, P., and F. Berthet. An investigation of human body model morphing for the assessment of abdomen responses to impact against a population of test subjects. *Traffic Inj Prev* 18:S142–s147, 2017.
- ⁹Brumblow M. L. and D. S. Zuby. Impact and injury patterns in frontal crashes of vehicles with good ratings for frontal crash protection. In: *21st ESV Conference* 2009.
- ¹⁰Cavanaugh, J. M. The biomechanics of thoracic trauma. *Accidental Injury*, New York: Springer, 1993, pp. 362–390.
- ¹¹Crandall, J. R., D. Lessley, G. Shaw, and J. Ash. Displacement response of the spine in restrained PMHS during frontal impacts. *Int. J. Automot. Eng.* 5:59–64, 2014.
- ¹²Davis, M. L., B. Koya, J. M. Schap, and F. S. Gayzik. Development and full body validation of a 5th percentile female finite element model. *Stapp Car Crash J.* 60:509–544, 2016.
- ¹³DeWit, J. A., and D. S. Cronin. Cervical spine segment finite element model for traumatic injury prediction. *J. Mech. Behav. Biomed. Mater.* 10:138–150, 2012.
- ¹⁴Fice, J. B., D. S. Cronin, and M. B. Panzer. Cervical spine model to predict capsular ligament response in rear impact. *Ann. Biomed. Eng.* 39:2152–2162, 2011.
- ¹⁵Gayzik, F. S., I. P. Marcus, K. A. Danelson, J. D. Rupp, C. R. Bass, N. Yoganandan, and J. Zhang. A point-wise

- normalization method for development of biofidelity response corridors. *J. Biomech.* 48:4173–4177, 2015.
- ¹⁶Gayzik, F., D. Moreno, K. Danelson, C. McNally, K. Klinich, and J. D. Stitzel. External landmark, body surface, and volume data of a mid-sized male in seated and standing postures. *Ann. Biomed. Eng.* 40:2019–2032, 2012.
- ¹⁷Gayzik, F. S., D. M. Moreno, C. P. Geer, S. D. Wuertzer, R. S. Martin, and J. D. Stitzel. Development of a full body CAD dataset for computational modeling: a multi-modality approach. *Ann. Biomed. Eng.* 39:2568–2583, 2011.
- ¹⁸Gehre C., H. Gades and P. Wernicke. Objective rating of signals using test and simulation responses. In: *21st International Technical Conference on the Enhanced Safety of Vehicles Conference (ESV)*, Stuttgart, Germany, 2009, pp. 15–18.
- ¹⁹Guleyupoglu B., R. Barnard and F. S. Gayzik. Automating Regional Rib Fracture Evaluation in the GHBMDC Detailed Average Seated Male Occupant Model. SAE Technical Paper, 2017.
- ²⁰Hayes, A. R. Geometric and Kinematic Validation Studies in the Thoracic and Abdominal Regions of a Detailed Human-Body Finite Element Model. Winston-Salem: Wake Forest University, 2013.
- ²¹Hayes, A. R., N. A. Vavalle, D. P. Moreno, J. D. Stitzel, and F. S. Gayzik. Validation of simulated chestband data in frontal and lateral loading using a human body finite element model. *Traffic Inj. Prev.* 15:181–186, 2014.
- ²²Kim, Y. H., J. E. Kim, and A. W. Eberhardt. A new cortical thickness mapping method with application to an in vivo finite element model. *Comput. Methods Biomech. Biomed. Eng.* 17:997–1001, 2012.
- ²³Lee, E. L., M. Craig, and M. Scarboro. Real-world rib fracture patterns in frontal crashes in different restraint conditions. *Traffic Inj. Prev.* 16(Suppl 2):S115–123, 2015.
- ²⁴Lessley, D., G. Shaw, J. Ash, and J. R. Crandall. A Methodology for Assessing Intrasegmental Kinematics of the Whole Human Spine during Impacts. *Int. J. Automot. Eng.* 5:1–6, 2014.
- ²⁵Li, Z., M. W. Kindig, J. R. Kerrigan, C. D. Untaroiu, D. Subit, J. R. Crandall, and R. W. Kent. Rib fractures under anterior–posterior dynamic loads: experimental and finite-element study. *J. Biomech.* 43:228–234, 2010.
- ²⁶Li, Z., M. W. Kindig, D. Subit, and R. W. Kent. Influence of mesh density, cortical thickness and material properties on human rib fracture prediction. *Med. Eng. Phys.* 32:998–1008, 2010.
- ²⁷Maltese, M. R., R. H. Eppinger, H. H. Rhule, B. R. Donnelly, F. A. Pintar, and N. Yoganandan. Response corridors of human surrogates in lateral impacts. *Stapp Car Crash J.* 46:321–351, 2002.
- ²⁸Mao, H., L. Zhang, B. Jiang, V. V. Genthikatti, X. Jin, F. Zhu, R. Makwana, A. Gill, G. Jandir, and A. Singh. Development of a finite element human head model partially validated with thirty five experimental cases. *J. Biomech. Eng.* 135:111002, 2013.
- ²⁹Mattucci, S. F., J. A. Moulton, N. Chandrashekar, and D. S. Cronin. Strain rate dependent properties of younger human cervical spine ligaments. *J. Mech. Behav. Biomed. Mater.* 10:216–226, 2012.
- ³⁰Mattucci, S. F., J. A. Moulton, N. Chandrashekar, and D. S. Cronin. Strain rate dependent properties of human craniovertebral ligaments. *J. Mech. Behav. Biomed. Mater.* 23:71–79, 2013.
- ³¹2016 Fatal motor vehicle crashes: Overview. edited by N. C. f. S. a. Analysis. Washington DC: National Highway Traffic Safety Administration, 2017.
- ³²Panjabi, M. M., J. J. Crisco, A. Vasavada, T. Oda, J. Cholewicki, K. Nibu, and E. Shin. Mechanical properties of the human cervical spine as shown by three-dimensional load–displacement curves. *Spine* 26:2692–2700, 2001.
- ³³Park G., T. Kim, J. R. Crandall, C. Arregui-Dalmases and J. Luzon-Narro. Comparison of Kinematics of GHBMDC to PMHS on the Side Impact Condition. In: *International Research Council on Biomechanics of Injury*. Gothenburg, Sweden: 2013.
- ³⁴Pattimore, D., P. Thomas, and S. Dave. Torso injury patterns and mechanisms in car crashes: an additional diagnostic tool. *Injury* 23:123–126, 1992.
- ³⁵Pietsch, H. A., K. E. Bosch, D. R. Weyland, E. M. Spratley, K. A. Henderson, R. S. Salzar, T. A. Smith, B. M. Sagara, C. K. Demetropoulos, C. J. Dooley, and A. C. Merkle. Evaluation of WIAMan Technology Demonstrator Biofidelity Relative to Sub-Injurious PMHS Response in Simulated Under-body Blast Events. *Stapp Car Crash J.* 60:199–246, 2016.
- ³⁶Poulard, D., R. Kent, M. Kindig, Z. Li, and D. Subit. Thoracic response targets for a computational model: A hierarchical approach to assess the biofidelity of a 50th-percentile occupant male finite element model. *J. Mech. Behav. Biomed. Mater.* 45:45–64, 2015.
- ³⁷Poulard, D., D. Subit, B. Nie, J.-P. Donlon, and R. W. Kent. The contribution of pre-impact posture on restrained occupant finite element model response in frontal impact. *Traffic Inj. Prev.* 16:S87–S95, 2015.
- ³⁸Schoell, S. L., A. A. Weaver, J. E. Urban, D. A. Jones, J. D. Stitzel, E. Hwang, M. P. Reed, and J. D. Rupp. Development and validation of an older occupant finite element model of a mid-sized male for investigation of age-related injury risk. *Stapp Car Crash J.* 59:359, 2015.
- ³⁹Shaw, G., D. Parent, S. Purtsezov, D. Lessley, J. Crandall, R. Kent, H. Guillemot, S. A. Ridella, E. Takhounts, and P. Martin. Impact response of restrained PMHS in frontal sled tests: skeletal deformation patterns under seat belt loading. *Stapp Car Crash J.* 53:1, 2009.
- ⁴⁰Shi, X., L. Cao, M. P. Reed, J. D. Rupp, and J. Hu. Effects of obesity on occupant responses in frontal crashes: a simulation analysis using human body models. *Comput. Methods Biomech. Biomed. Eng.* 18:1280–1292, 2015.
- ⁴¹Shin, J., and C. Untaroiu. Biomechanical and injury response of human foot and ankle under complex loading. *J. Biomech Eng* 135:101008, 2013.
- ⁴²SAE. Instrumentation for Impact Test—Part 1—Electronic Instrumentation. J211/1, Warrendale, PA: Society of Automotive Engineers Test Instrumentation Standards Committee, 1995.
- ⁴³SAE. Sign convention for vehicle crash testing. J1733, Warrendale, PA: Society of Automotive Engineers Test Instrumentation Standards Committee, 1995.
- ⁴⁴Soni, A., and P. Beillas. Modelling hollow organs for impact conditions: a simplified case study. *Comput. Methods Biomech. Biomed. Eng.* 18:730–739, 2013.
- ⁴⁵Takhounts, E. G., M. J. Craig, K. Moorhouse, J. McFadden, and V. Hasija. Development of brain injury criteria (Br IC). *Stapp Car Crash J.* 57:243–266, 2013.
- ⁴⁶Untaroiu, C. D., N. Yue, and J. Shin. A finite element model of the lower limb for simulating automotive impacts. *Ann. Biomed. Eng.* 41:513–526, 2013.

- ⁴⁷Vavalle, N. A., M. L. Davis, J. D. Stitzel, and F. S. Gayzik. Quantitative validation of a human body finite element model using rigid body impacts. *Ann. Biomed. Eng.* 43:2163–2174, 2015.
- ⁴⁸Vavalle, N. A., B. C. Jelen, D. P. Moreno, J. D. Stitzel, and F. S. Gayzik. An evaluation of objective rating methods for full-body finite element model comparison to PMHS tests. *Traffic Inj. Prev.* 14:S87–S94, 2013.
- ⁴⁹Vavalle N., D. Moreno, A. Rhyne, J. Stitzel and F. Gayzik. The validation of a full body finite element model in lateral full body sled and drop tests. In: *VT-WFU School of Biomedical Engineering and Sciences Symposium, Winston-Salem, NC*, 2012.
- ⁵⁰Vavalle, N. A., D. P. Moreno, A. C. Rhyne, J. D. Stitzel, and F. S. Gayzik. Lateral impact validation of a geometrically accurate full body finite element model for blunt injury prediction. *Ann. Biomed. Eng.* 41:497–512, 2013.
- ⁵¹Vavalle, N. A., A. B. Thompson, A. R. Hayes, D. P. Moreno, J. D. Stitzel, and F. S. Gayzik. Investigation of the mass distribution of a detailed seated male finite element model. *J. Appl. Biomech.* 30:471–476, 2014.
- ⁵²World Health Organization. Global Status Report on Road Safety. Geneva: World Health Organization, 2015.
- ⁵³Yanaoka T. and Y. Dokko. A Parametric Study of Age-Related Factors Affecting Intracranial Responses under Impact Loading Using a Human Head/Brain FE Model. In: *International Research Council on Biomechanics Injury (IRCOBI)*. Gothenburg, Sweden: 2013.
- ⁵⁴Yue N., J. Shin and C. Untaroiu. Development and validation of an occupant lower limb finite element model. In: *SAE Technical Paper*, 2011.
- ⁵⁵Yue, N., and C. D. Untaroiu. A numerical investigation on the variation in hip injury tolerance with occupant posture during frontal collisions. *Traffic Inj. Prev.* 15:513–522, 2014.